Frontiers in Bioscience Elite

Front. Biosci. (Elite Ed) **2022**; 14(3): 17
https://doi.org/10.31083/j.fbe1403017

Original Research

Ferritin Iron Responsive Elements (IREs) mRNA Interacts with eIF4G and Activates *In Vitro* Translation

Mateen A. Khan[1,2,*]

[1]Department of Chemistry and Biochemistry, Hunter College of the City University of New York, New York, NY 10065, USA
[2]Department of Life Science, College of Science & General Studies, Alfaisal University, 11533 Riyadh, Saudi Arabia
*Correspondence: matkhan@alfaisal.edu; makhan@hunter.cuny.edu (Mateen A. Khan)
Academic Editors: Guoyao Wu and William Konigsberg
Submitted: 18 October 2021 Revised: 17 April 2022 Accepted: 11 May 2022 Published: 4 July 2022

Abstract

Background: Eukaryotic initiation factor (eIF) 4G plays an important role in assembling the initiation complex required for ribosome binding to mRNA and promote translation. Translation of ferritin IRE mRNAs is regulated by iron through iron responsive elements (IREs) and iron regulatory protein (IRP). The noncoding IRE stem-loop (30-nt) structure control synthesis of proteins in iron trafficking, cell cycling, and nervous system function. High cellular iron concentrations promote IRE RNA binding to ribosome and initiation factors, and allow synthesis of ferritin. **Methods**: *In vitro* translation assay was performed in depleted wheat germ lysate with supplementation of initiation factors. Fluorescence spectroscopy was used to characterize eIF4F/IRE binding. **Results**: Eukaryotic initiation factor eIF4G increases the translation of ferritin through binding to stem loop structure of iron responsive elements mRNA in the 5′-untranslated region. Our translation experiment demonstrated that exogenous addition of eIF4G selectively enhanced the translation of ferritin IRE RNA in depleted WG lysate. However, eIF4G facilitates capped IRE RNA translation significantly higher than uncapped IRE RNA translation. Addition of iron with eIF4G to depleted WG lysate significantly enhanced translation for both IRE mRNA (capped and uncapped), confirming the contribution of eIF4G and iron as a potent enhancer of ferritin IRE mRNA translation. Fluorescence data revealed that ferritin IRE strongly interacts to eIF4G (K_d = 63 nM), but not eIF4E. Further equilibrium studies showed that iron enhanced (~4-fold) the ferritin IRE binding to eIF4G. The equilibrium binding effects of iron on ferritin IRE RNA/eIFs interaction and the temperature dependence of this reaction were measured and compared. The K_d values for the IRE binding to eIF4G ranging from 18.2 nM to 63.0 nM as temperature elevated from 5 °C to 25 °C, while the presence of iron showed much stronger affinity over the same range of temperatures. Thermodynamic parameter revealed that IRE RNA binds to eIF4G with $\Delta H = -42.6 \pm 3.3$ kJ. mole^{-1}, $\Delta S = -11.5 \pm 0.4$ J. mole^{-1}K^{-1}, and $\Delta G = -39.2 \pm 2.7$ kJ. mole^{-1}, respectively. Furthermore, addition of iron significantly changed the values of thermodynamic parameters, favoring stable complex formation, thus favoring efficient protein synthesis. This study first time demonstrate the participation of eIF4G in ferritin IRE mRNA translation. **Conclusions**: eIF4G specifically interacts with ferritin IRE RNA and promotes eIF4G-dependent translation.

Keywords: eukaryotic initiation factor; fluorescence; IREs; *in vitro* translation; protein-RNA interaction; thermodynamics

1. Introduction

Cellular iron level regulates the expression of iron encoded proteins by iron responsive elements (IREs) mRNA at 5′-untranslated region (UTR). IREs are present in either the 3′-UTR or 5′-UTR. Based on the IREs location at untranslated region of target mRNA, iron regulatory proteins (IRPs) act as a post-transcriptional modulator of mRNA encoding protein [1,2]. Ferritin protein synthesis requires the interaction of stem-loops structures of IREs-mRNA in the 5′-UTR with IRP1. 30-nts stem-loop structure of IREs is highly conserved. The stem is stabilized by upper helix base pairing and a pseudo-tri loop with sequence CAGUGX (C denoted A, C or U), lower helix cytosine bulge and an asymmetric loop [1,3]. Iron can have opposite metabolic effect; acts as either translational enhancer or repressor based on the location of IRE either 3′- or 5′-UTR [4]. Studies reported that removal of the IREs stem-loop structure leads to the IRP independent translation [4]. Disturbance in cellular iron concentration can destabilizes IRE-IRP interaction which leads to either enhanced translation or inhibit translation of iron regulatory, iron transport, and iron storage proteins [5]. Therefore, the elevated iron levels in brain cells destabilize the IRE-dependent signaling pathway which directly or indirectly contributes to the Alzheimer's amyloid precursor protein aggregation and neuronal loss in Alzheimer's diseases [6,7]. Iron balance is critical at cellular level as well as systemic level and mis-regulation of iron can lead to oxidative damage and cell death including Alzheimer's disease, Parkinson's disease, Friedreich's ataxia, multiple sclerosis and neuroferritinopathy [8–10]. It has been reported that high iron in the brain can cause several disorders in the central nervous system. Elevated level of iron has been observed in the brain of Alzheimer's patients [11,12]. This high iron accumulation in the amyloids of Alzheimer's patients leads to disrupt the complex formation between iron responsive elements and iron regulatory proteins, which leads to the alterations in the storage and transport of iron [5,13].

Copyright: © 2022 The Author(s). Published by IMR Press.
This is an open access article under the CC BY 4.0 license.

Publisher's Note: IMR Press stays neutral with regard to jurisdictional claims in published maps and institutional affiliations.

Translation initiation in eukaryotes requires the concerted effort of several eIFs. Among the protein complexes required is the cap binding complex, eIF4F. Initiation include series of events that initiate with the interaction of 5′-cap moiety of mRNA with eIF4F [14,15]. Eukaryotic translation initiation factor eIF4F is comprised of subunits eIF4E, eIF4G, and eIF4A. Interaction of RNA with eIF4E and eIF4G are the key factors for initiation of protein synthesis. The small subunit eIF4E interacts with 5′-mRNA cap structure; eIF4A unwinds secondary structure of mRNA at 5′-UTR to promote the binding of ribosome [16]. The subunit eIF4G is a large multidomain protein interacts with several other translation initiation factors on the 5′-leader sequences to promote scanning of 40S ribosome to the correct AUG initiation codon and start mRNA translation [17,18]. Functional domains of eIF4G contains several binding sites for RNA and other eIFs [14,19,20], which is largely responsible for ribosome attachment, mRNA circularization and enhancing efficiency of mRNA translation through many protein and RNA interactions. Previously we have shown that IRE RNA binds to eIF4F and IRP1 protein [4,21–23]. Further iron enhances the interactions between eIF4F with IRE RNA and simultaneously increases translation via inhibiting IRP/IRE RNA interactions. To further examine the role of eIF4G in translation, we investigated the interaction between ferritin IRE RNA and eIF4G and correlate the binding affinity with translational efficiency. We demonstrated that ferritin IRE RNA strongly binds to eIF4G but not eIF4E. Moreover, addition of exogenous eIF4G in depleted wheat germ lysate significantly enhanced ferritin IRE mRNA translation *in vitro*.

2. Materials and Methods

2.1 Materials

30-nucleotide (sequence: 5′-GUUCUUGCUUCAACAGUGUUUGAACGGAAC-3′) ferritin IRE mRNA and 5S RNA 30-nt (5′-UAGUACUUGGAUGGGAGACCGCCUGGGA AU-3′) were purchase from Metabion. Preparation of RNAs were performed as described in references [21,24]. The concentrations of ferritin IRE RNA and 5S RNA solutions were determined by measuring the optical density at $\lambda_{260\ nm}$ spectrophotometrically. Recombinant protein of human eukaryotic translation initiation factors eIF4G1 (Catalog-TP312877, Lot-107AB8) and eIF4E (Catalog-TP721168, Lot-0330637) were supplied by OriGene Co. (Rockville, MD). Proteins expressed and purified from mammalian cells using HeK293T cells, a line derived from human embryonic kidney. Proteins are purified using an anti-DDK immunoaffinity column followed by conventional chromatography steps as described in OriGene protocols. Human eIF4E and eIF4G1 stock solutions were prepared by dissolving fix amount of protein crystals in 1 mL of 20 mM HEPES/KOH buffer, pH 7.2, and its concentrations were measured spectrophotometrically using Bradford method. Ferritin mRNA construct was transcribed and purified as described previously [25]. Capped mRNA was synthesized by using the Ribo m^7G cap analog reaction protocol provided by Promega. Under optimized conditions, above 95% RNA was capped. Wheat germ lysate was supplied by Promega. Wheat germ lysate contain all the cellular components necessary for protein synthesis.

2.2 In Vitro Translation Assay

Ferritin mRNA transcript (capped and uncapped) were translated in wheat germ (WG) lysate and depleted wheat germ (WG) lysate as described previously [4,26]. Translation assay of depleted WG lysate is dependent on the supplementation of eIF4G and eIF4E. eIF4F depleted WG lysate were prepared following Promega instructions manual. WG lysate (200 μL) was mixed to m^7GTP-Sepharose (300 μL) and incubated with continuous rotation for half an hour at 5 °C. The column was washed with standard buffer: 20 mM HEPES/KOH (pH 7.2), and eukaryotic initiation factors eluted with above buffer containing 100 mM GTP. The extent of depletion of the eIF4G and eIF4E from wheat germ lysate was determined by Western blot analysis following resolution of the extract by SDS-PAGE as shown previously [27]. Western blot analysis confirmed that the level of eIF4G and eIF4E was reduced by about 95%. Capped and uncapped transcript mRNA (IRE luciferase reporter mRNA) was assayed with WG lysate and depleted WG lysate according to the manufacture instructions. For all reaction mixture transcript RNA (capped and uncapped) was heated at 85 °C for 15 min, and the reaction mixture annealed slowly at room temperature for 30 min. When iron was added, all sample incubations were anaerobic. Anaerobiosis conditions for iron was achieved with using argon in a glass sealed vials as previously described [21]. Briefly, 50 (l reaction mixture included 10 μg ferritin IRE-*luc* mRNA template; 25 μL of either WG lysate or depleted WG lysate; 1 mM amino acids (set of 19 amino acids); 40 units of RNasin Ribonuclease, 100 mM potassium chloride; 2 mM magnesium chloride [28,29]. Incubation of titration mixture was for 120 min at 25 °C. depleted WG lysate translation is dependent upon addition of eIF4G (100 nM) and eIF4E (100 nM). To investigate the eIF4G-dependent translation, depleted WG lysate was added with 100 nM eIF4G or eIF4E in translation reaction mixture. Translation was also assayed with addition of Fe^{2+} (50 micro M). When Fe^{2+} was used, experiments were anaerobic conditions. Nitrogen-purged solution of 0.1 M HCl used to dissolve $FeSO_4$ as described previously [21]. After addition of the luciferase assay reagent (100 μL) to each translation sample, the amount of protein expression was determined by measuring the light produced by Luminometer at 495 nm. Control sample containing no RNA, were used to measurement of any background absorbance.

IMR Press

2.3 Fluorescence Measurements

The titration experiments for the ferritin IRE RNA interaction with eIF4G, eIF4E or eIF4G·eIF4E complex were performed by fluorescence intensity measurements as previously described [30]. Protein fluorescence was excited at λ_{Ex} 280 nm, and the data was collected at λ_{Em} of 340 nm. Titration experiments were performed for 0.1 μM eIF4G, eIF4E, or eIF4G·eIF4E complex with addition of different amount ferritin IRE in steady-state conditions provided by pre-incubation in standard buffer 20 mM HEPES/KOH (pH 7.2), at ionic strength of 100 mM KCl, 2 mM $MgCl_2$, and 5% (v/v) glycerol. The binding of eIF4G and eIF4E with ferritin IRE RNA were measured by quenching of intrinsic fluorescence of protein. The reaction mixture was thermostat, and the cuvette temperature was maintained (ΔT $\pm$ 0.2 °C) for all temperature-dependent binding experiments. Before the fluorescence measurements, the samples were incubated for 20 min at appropriate temperature. Binding of eIF4G, eIF4E, or eIF4G·eIF4E with ferritin IRE RNA were determined by measuring the intrinsic fluorescence intensity of eIFs protein and protein-IRE RNA solution. Normalized fluorescence ($\Delta F/\Delta F_{max}$) between eIFs-IRE complex and individual eIFs intrinsic fluorescence intensity were used to measure the dissociation constant (K_d) as described previously [30,31]. In control experiments, fluorescence intensity of eIFs (0.1 μM) alone was measured. In another sample fluorescence intensity of ferritin IRE RNA at specific concentration was measured. Control fluorescence intensity was used to determine the corrected fluorescence intensity of the complex. The fluorescence data obtained above were corrected for dilution and blank contributions, if any, as described previously [27]. All solutions were filtered prior to the measurements. The fluorescence spectra are the average of three individual spectrum. The fluorescence data were fit by means of nonlinear least squares method, using Kaleida-Graph Software (Version 2.1.3; Synergy Abelbeck Software Inc. USA)

2.4 Binding Sites Measurements

The number of IRE binding site on the eukaryotic initiation factor eIF4G were measured by exciting the protein and protein-RNA complex at λ_{max} 280 nm and fluorescence intensity was recorded at emission λ_{max} 340 nm. Protein (eIF4G) fluorescence quenching was measured with addition of varying amount of ferritin IRE RNA. For each molar ratio of RNA/eIF4G, relative fluorescence change compared to control (untreated eIF4G fluorescence) were recorded. The fluorescence intensity of protein (F) as a function of ferritin IRE RNA experimental data was fitted according to the following equation: $Q = (F_0 - F)/m$. where Q and m are the fractional and maximal quench of eIF4G protein with and without addition of RNA. Fractional quench (Q) of eIF4G is directly related with RNA binding following equation $Q = [\text{eIF4G-IRE}]/[\text{eIF4G}]_T$, where $[\text{eIF4G}]_T$ is the total amount of protein in solution. Q is related to the equilibrium concentration of the ratio of eIF4G/IRE complex and eIF4G total. The resulting data were expressed as number of binding sites for IRE on eIF4G as described previously using the Scatchard analysis [30,32,33]. K_a values were obtained from the Scatchard plot and nonlinear least square fitting were similar. The fluorescence data were fit to nonlinear least square using Kaleida Graph software (Version 2.1.3; Synergy Abelbeck Software Inc. USA).

2.5 Competitive Binding Studies

For competitive binding measurements, the molar ratio of eIF4G to eIF4E was 1:0, 1:1, and 1:2. eIF4G concentration was kept constant at 0.1 μM. Titration were performed at several eIF4E concentrations (0.0, 100, and 200 nM) as a function of IRE in steady state conditions, provided by pre-incubation of titration samples for 15 min. Titration experiments were performed in standard buffer (20 mM HEPES/KOH, pH 7.2) containing 100 mM KCl and 2 mM $MgCl_2$. Fluorescence change of eukaryotic initiation factor eIF4G with increasing concentrations of IRE-mRNA were recorded by spectroscopic measurements. For eIF4G/IRE binding measurements the excitation and emission λ_{max} 280 nm (slit width 4 nm) and 332 nm (slit width 5 nm) were used by observing the fluorescence signal change of the eIF4G protein and protein/RNA complex solution. The data were fit by non-linear least-square using Kaleida Graph software. The characteristic of competitive and uncompetitive binding was determined from the Lineweaver-Burk plot as described previously [4,30].

2.6 Thermodynamic Parameters from van't Hoff Analysis

Temperature dependence of dissociation constant were used to construct van't Hoff plots according to the equation:

$$\ln K_a = -[\Delta H]/[RT] + + [\Delta S]/[R] \quad (1)$$

where K_a is the binding affinity at each temperature (5, 10, 15, 20, and 25 °C). The entropy changes ΔS and enthalpy change ΔH were calculated using the intercept and slope of $\ln K_a$ *versus* temperature (T^{-1}). The change in free energy ΔG of the binding reaction was calculated at 25 °C by the following equation:

$$\Delta G = \Delta H - T\Delta S \quad \text{and} \quad \Delta G = -RT \ln K_a \quad (2)$$

3. Results

3.1 eIF4G-Dependent Translation of Ferritin IRE mRNA

We have previously [4] shown that ferritin IRE interacts with eIF4F, but functional differences between two subunits of eIF4F, eIF4G and eIF4E in protein synthesis and specificity binding has not been elucidated. We have correlated the binding affinity with translation efficiency of individual subunits. To determine whether the two subunits

eIF4G and eIF4E were able to support capped or uncapped ferritin luciferase mRNA translation in eIF4F-dependent WG lysate was prepared [34]. eIF4F-depleted lysate was generated by binding of WG extract to m^7GTP-Sepharose. Western blot analysis confirmed that the level of eIF4G and eIF4E was reduced by 95%. To assess the capped/uncapped ferritin mRNA translation, we used a complete WG lysate and depleted WG lysate that was supplemented with the subunits eIF4G and/or eIF4E initiation factors. Depletion of eIF4F from the wheat germ lysate reduced translation by more than 95% (compare WG lysate and depleted WG lysate translation) (Figs. 1,2). Adding capped or uncapped ferritin mRNA to a complete wheat germ lysate significantly enhanced protein synthesis. However, addition of capped or uncapped ferritin IRE RNA to depleted lysate of wheat germ did not support translation *in vitro* (Fig. 1). Supplementation of eIF4G to depleted wheat germ lysate enhanced translation of capped and uncapped ferritin mRNA up to 51- and 40-fold (Fig. 1), whereas supplementation of eIF4E to the lysate of DWG did not appear translational difference of capped and uncapped ferritin IRE mRNA. As shown in Fig. 1, the addition of both subunits eIF4G and eIF4E (mixed complex) can fully support translation of ferritin mRNA. Interestingly, translation efficiency appears to correlate more closely with eIF4G than eIF4E subunit. Furthermore, wheat germ translation was largely dependent on eIF4G. Translation results suggest that capped/uncapped mRNA provides eIF4G-dependent translation, whereas capped mRNA facilitates high level of translation as compared to uncapped mRNA through eIF4G binding. Moreover, Addition of iron and eIF4G to depleted wheat germ lysate increases translation ~2-fold for both ferritin mRNA.

To examine the effect of inhibitor (IRP1), on the translation of capped/uncapped ferritin IRE RNA, eIF4G, eIF4E-depleted lysate was program to determine the degree to which translation was inhibited. The results showing (Fig. 3) that IRP1 inhibits translation of ferritin IRE RNA both in complete WG lysate and depleted WG lysate supplemented with eIF4G. Addition of 100 nM IRP1 inhibited 40–45% *in vitro* translation from capped/uncapped mRNA was observed in complete WG lysate, whereas 40–50% inhibition was observed in depleted WG lysate supplemented with eIF4G. These data suggest that IRP1 preferentially binds to ferritin IRE RNA as a result translation inhibited. Further, addition of 50 (M Fe^{2+} in DWG lysate supplemented with eIF4G restored translation by 90% for capped/uncapped mRNA by stabilizing eIF/IRE RNA complex [4] and destabilizing IRP1/IRE RNA complex to promote translation [21]. Iron reversed IRP1 inhibition of protein synthesis (Fig. 3A and B) by inducing release of IRP1 from IRE RNA and promote eIFs binding. Increasing cellular iron concentrations will lower IRP1/IRE RNA affinity and higher eIF4G binding, ribosome assembly, and ferritin mRNA translation.

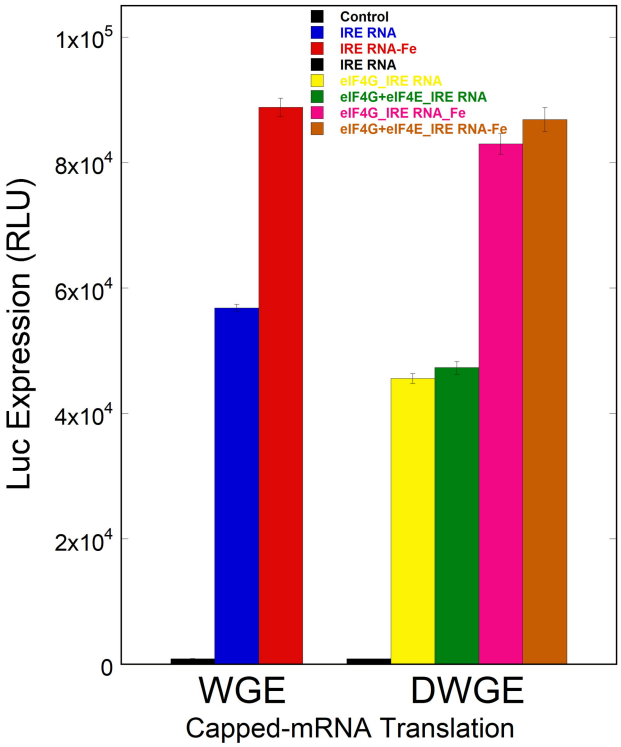

Fig. 1. eIF4G enhances capped ferritin IRE translation in eIF4F-depleted wheat germ extract. Translation assay of WG lysate and depleted WG lysate contain 10 g mRNA (capped). Depleted WG lysate was supplemented with 100 nM eIF4G or eIF4E. Concentration of Fe^{2+} was 50 μM. Point represents the average of three experiments, and the error bars are indicated.

To assess the initiation factor concentration on the translation, we performed translation experiments with different amount of eIF4G or eIF4E with both capped and uncapped ferritin IRE-RNA in depleted WG lysate. As the concentration of eIF4G was increased translation of ferritin mRNA was enhanced irrespective of capped/uncapped IRE RNA (Fig. 4). Supplementation of 50 nM eIF4G enhanced 58-fold of translation for the capped IRE RNA (Fig. 4) and 54-folds of translation for uncapped IRE RNA in WG lysate. In contrast, supplementation of eIF4E did not produce any significant change on translation level of either capped or uncapped ferritin IRE RNA. As eIF4E cannot bind to ferritin IRE RNA and eIF4G strongly interacts with IRE RNA, these data appear to correlate more closely with translational efficiency with eIF4G rather than the cap binding to eIF4E. We observed that eIF4G increased cap-dependent translation efficiency to a higher level than the uncapped IRE mRNA translation. Supplementation of exogenous eIF4G initiation factor to the depleted wheat germ lysate resulted in 85% recovery of *in vitro* translation of ferritin mRNA, confirming that eIF4G specifically recognizes the ferritin mRNA. Furthermore, addition of iron increases the eIF4G·IRE RNA binding affinity as illustrated by enhanced protein synthesis, resulted from iron being added to

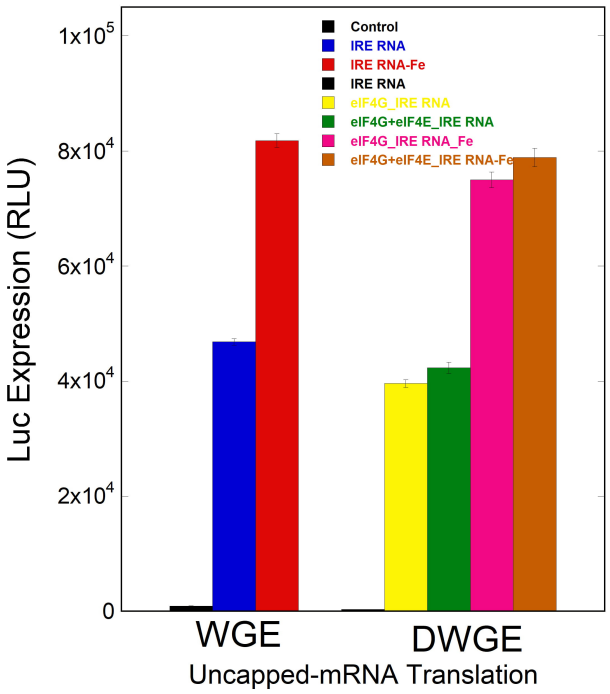

Fig. 2. Translation assay of uncapped ferritin IRE with eIF4G. Uncapped ferritin mRNA (10 g) was assayed in WG lysate and depleted WG lysate. Depleted WG lysate was supplemented with eIF4G (100 nM) and Fe^{2+} 50 (M), respectively. Each uncapped mRNA represents the average of three experiments, and the error bars are reported.

the wheat germ lysate along with exogenous eIF4G. These results strongly suggest that iron and eIF4G plays a key part in enhancing protein synthesis of ferritin regulatory elements mRNA.

3.2 Interaction of Ferritin IRE with eIF4G

The binding affinity of ferritin IRE RNA with large subunit eIF4G was measured to assess the specificity of complex formation. As shown in Fig. 5, eIF4G fluorescence was presented with increasing amounts of IRE RNA. Fluorescence data indicated that about 80% quenching of eIF4G fluorescence intensity with addition of ferritin IRE at the highest molar ratios. The amount of eIF4G fluorescence change is proportional to concentration of ferritin IRE-RNA binding. Fig. 5 inset indicated corresponding Scatchard plot for the eIF4G/IRE binding. Binding affinity (K_a) and number of binding site (n) of IRE RNA to eIF4G was measured by the slope and intercept of a Scatchard plot (Q/IRE] $\times$ 10^{-6} *vs* Q). The K_a and n for the interaction of ferritin IRE to eIF4G were 14.8 $\times$ 10^6 M^{-1} and 1.0. These results suggest that eIF4G contain one binding domain for IRE RNA. K_a values of ferritin IRE with eIF4G were calculated by non-linear least squares method (K_d = 63.0 nM) and Scatchard plot. Equilibrium values are reported in K_d and K_a, whereas $K_a = 1/K_d$. The results obtained by two-independent data analysis methods are in good agreement.

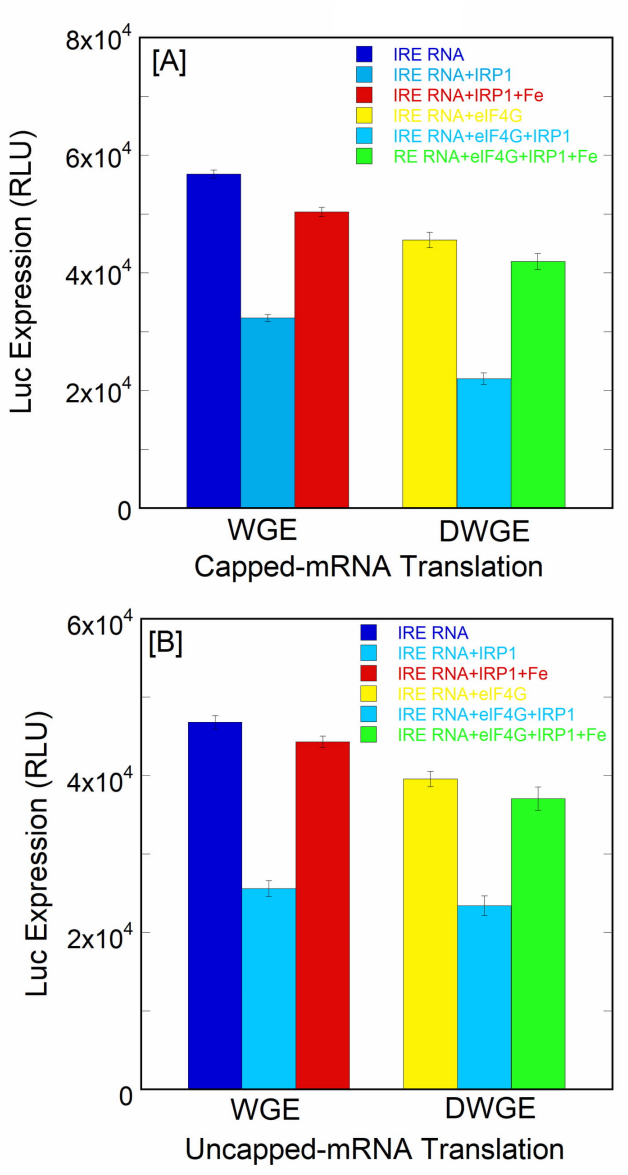

Fig. 3. Inhibition in translation of ferritin IRE mRNA in WG lysate and eIF4G-dependent lysate by IRP1. (A) Capped IRE RNA and (B) uncapped IRE RNA was translated in the WG lysate and depleted WG lysate. IRP1 concentration was 100 nM. Other conditions are shown in Fig. 1.

To assess the ability of IRE RNA binding to the subunits eIF4G and eIF4E, we determined the binding affinity of ferritin IRE with eIF4G, eIF4E, and eIF4G·eIF4E. eIF4G binds the ferritin IRE RNA with the dissociation constant (K_d) of 63 $\pm$ 4.3 nM (Fig. 6), similar to the binding of beta-globin mRNA [35] and several fold higher K_d than ferritin IRE RNA/eIF4F binding [4]. 5S RNA was used as a control under the same conditions to test for non-specific binding. Conversely, no binding of eIF4G with 30-oligonucleotide stem loop from yeast 5S RNA (a negative control) was detected (Fig. 6), suggesting that ferritin IRE-RNA specifically binds to subunit eIF4G, as re-

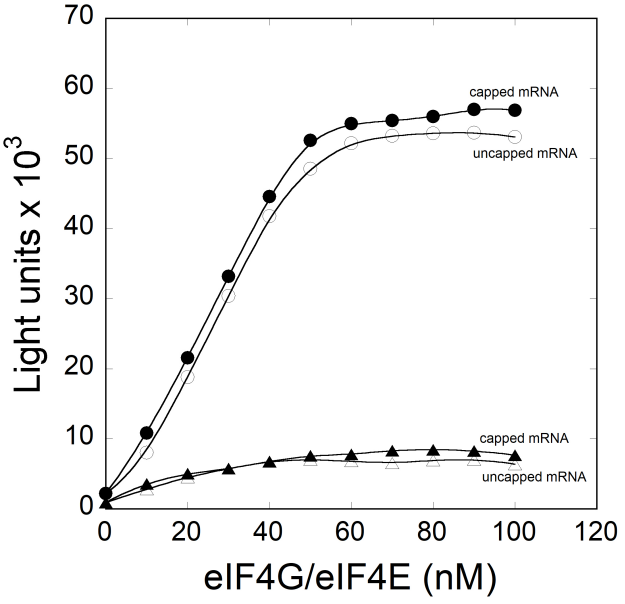

Fig. 4. eIF4G (but not eIF4E) supports *in vitro* translation (capped and uncapped) ferritin mRNA. Translation reaction contain eIF4F depleted wheat germ lysate with 10 (g) ferritin mRNA (capped or uncapped), and the indicated amount of recombinant eIF4G and eIF4E. Translation of capped (—●—) and uncapped (—○—) ferritin mRNA in depleted wheat germ extract supplemented with eIF4G; for capped (—▲—) and uncapped (—△—) ferritin mRNA translation in depleted wheat germ extract supplemented with eIF4E.

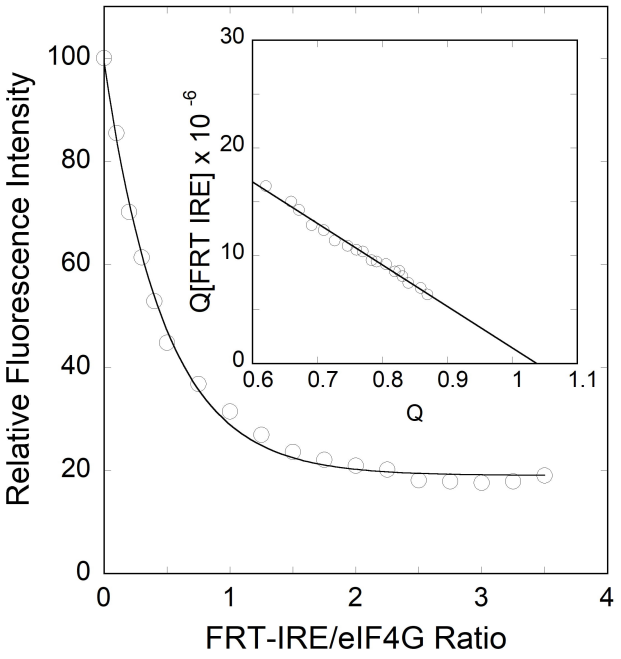

Fig. 5. Titration isotherm for the binding of eIF4G with varying ferritin IRE RNA. Binding isotherm of eIF4G (100 nM) was carried out in the presence of varying ferritin IRE concentrations (at 25 °C, $_{ex}$ = 280 nm, $_{em}$ = 332 nm). The *inset* showing the Scatchard plot of titration data for the interaction of IRE binding with eIF4G.

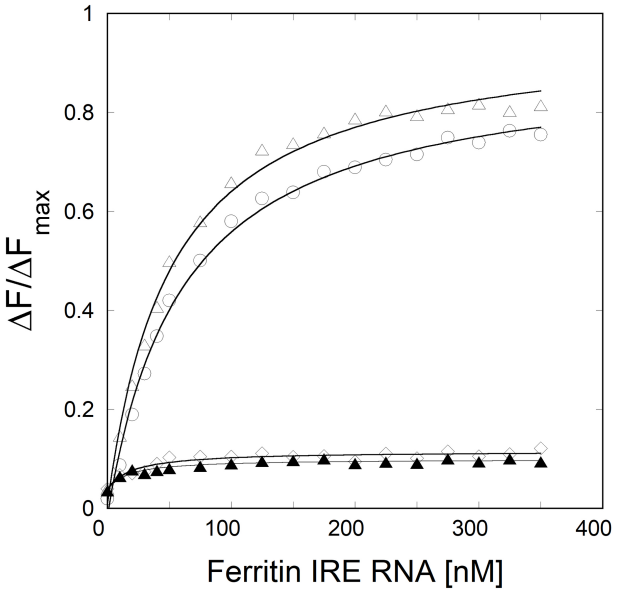

Fig. 6. Ferritin IRE RNA tightly binds to eIF4G. The normalized fluorescence values for the binding of eIF4G (—○—), eIF4G·eIF4E (—△—), and eIF4E (—◇—) versus concentration of ferritin IRE RNA. eIF4G (—▲—) did not bind a 5S RNA 30-oligonucleotide stem loop used as a negative control. eIF4G, eIF4E, and eIF4G·eIF4E concentration were 100 nM.

ported earlier for the binding of eIF4G with stem-loop structure from encephalomyocarditis viral RNA [35]. Strong binding of IRE-RNA with eIF4G, yet without the m^7G cap, explains the earlier examination that removing m^7G-cap from ferritin IRE does not affect the translation compared to the larger change on removing the IRE stem-loop structure [36]. The addition of eIF4E produced no significant difference on the interaction of ferritin IRE-RNA with eIF4G. However, eIF4E alone did not interact with ferritin IRE-RNA (Fig. 6). These results suggest that ferritin IRE RNA preferably binds to eIF4G, but not eIF4E. Moreover, equilibrium studies showed that iron enhanced ferritin IRE-RNA binding to eIF4G about 4-fold (eIF4G·IRE RNA-Fe^{2+}, K_d = 17.0 nM; eIF4G·IRE RNA, K_d = 63 nM) at 298K. On the other hand, addition of iron did not affect the binding affinity of eIF4E to ferritin IRE (Fig. 7). As eIF4E cannot bind to ferritin mRNA, while eIF4G strongly bind to ferritin mRNA, these results suggests that eIF4G enhances *in vitro* translation with depleted WG lysate by binding to ferritin mRNA.

To identify whether ferritin IRE RNA and eIF4E binding to eIF4G is competitive or uncompetitive, varying amount of ferritin mRNA and eIF4E were utilized. EIF4G protein fluorescence signal change was measured in the absence and presence of eIF4E with varying concentra-

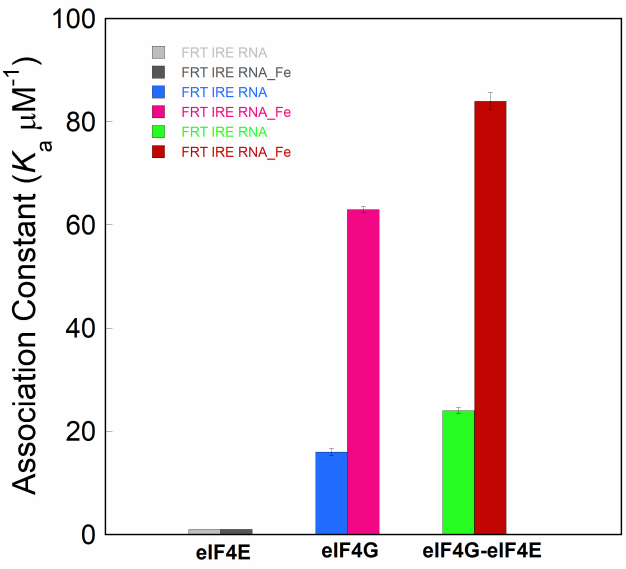

Fig. 7. Iron enhances the ferritin IRE binding to eIF4G. Histogram representation of affinity constant (K_a μM^{-1}) of ferritin IRE with eIF4E, eIF4G, and eIF4G·eIF4E with and without iron.

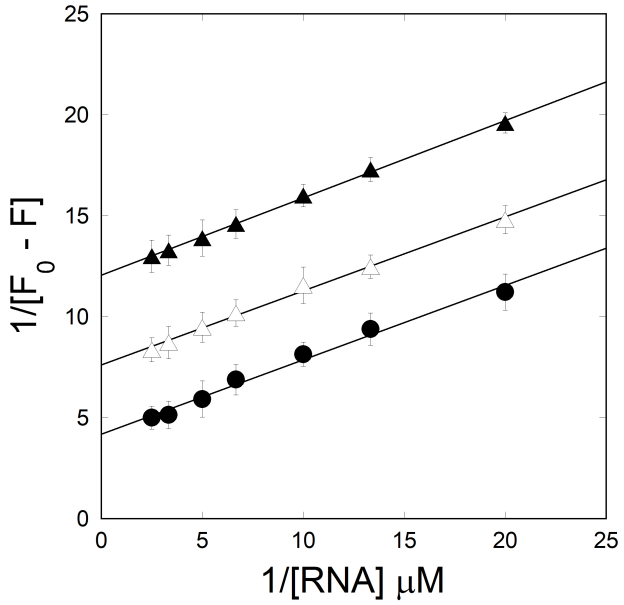

Fig. 8. Ferritin IRE and eIF4E binds noncompetitively to eIF4G. Change in fluorescence intensity of eIF4G (100 nM) as a function of ferritin IRE with addition of 0.0 nM eIF4E (—●—), 50 nM eIF4E (—△—), and 100 nM eIF4E (—▲—). Parallel lines of Lineweaver-Burk plots indicate uncompetitive.

tion of ferritin IRE-RNA. For ferritin IRE binding experiments, fluorescence titration results of the molar ratio of eIF4G:eIF4E was 1:0, 1:1, and 1:2, respectively. Changes in fluorescence intensity of eIF4G·eIF4E complex at different ferritin IRE-RNA concentrations were determined. As shown in Fig. 8, Lineweaver-Burk plots show that the binding of ferritin RNA and eIF4E to eIF4G is uncompetitive. However, IRP1 and eIF4F binds to ferritin IRE RNA competitively [4]. Fluorescence results revealed that ferritin IRE and eIF4E have different binding site on eIF4G.

3.3 Temperature Dependence Ferritin IRE/eIF4G Binding

The effect of temperature on eIF4G binding to ferritin IRE was observed by measuring the fluorescence intensity of protein and protein-RNA complex. The dissociation constant for eIF4G/IRE and eIF4G·eIF4E/IRE complexes with and without addition of iron was determine as a function of temperature by observing protein fluorescence quenching data. Fluorescence results at different temperatures revealed that the binding association of eIF4G/IRE and eIF4G·eIF4E/IRE complex enhanced with increased temperature. K_d values increased from 18.2 ± 1.1 nM to 63 ± 4.3 nM and 9.1 ± 0.3 nM to 46.3 ± 3.6 nM for the binding of eIF4G and eIF4G·eIF4E with IRE-RNA as temperature elevated from 5 °C to 25 °C (Table 1). Fluorescence result revealed that dissociation of eIF4G/IRE and eIF4G·eIF4E/IRE at 5 °C were higher as compared to 25 °C (Table 1). Addition of iron (50 μM Fe^{2+}) shows that eIF4G and eIF4G·eIF4E binding to ferritin IRE increased by about 4-time. Dissociation constant for the eIF4G/IRE and eIF4G(eIF4E/IRE with addition of Fe^{2+} increased to 17.0 ± 0.8 nM and 13.0 ± 0.5 nM at elevated temperature (25 °C, Table 1). Similarly, the dissociation of eIF4G/IRE and eIF4G(eIF4E/IRE complex in the presence of iron was lower at lower temperature (Table 1). The binding data shows that iron enhanced the binding of eIF4G and eIF4G(eIF4E with IRE at all temperatures (Table 1).

3.4 Thermodynamics of Ferritin IRE Binding to eIF4G

To examine the thermodynamic parameters for the binding of ferritin mRNA to eIF4G and eIF4G·eIF4E complex with and without addition of iron, temperature dependence equilibrium dissociation constant values were used. The equilibrium data was analyzed by the van't Hoff equation. Fig. 9 shows the $\ln K_{eq}$ *vs* T^{-1} plots for the binding of ferritin IRE with eIF4G and eIF4G(eIF4E in the absence and presence of iron. Thermodynamic parameters enthalpy and entropy change calculated using linear fitting of the plot. Data in Table 2 showing that thermodynamic parameters, ΔH, ΔS, and ΔG changes significantly for ferritin IRE RNA/eIFs complexes with the addition of iron. van't Hoff equation yielded the ΔH values for the association of eIF4G and eIF4G(eIF4E with IRE-RNA were –42.6 ± 3.3 kJ. mol^{-1} and –54.6 ± 4.3 J. $mol^{-1}K^{-1}$, respectively, whereas association is entropy opposed for both these complexes. Addition of iron to eIF4G(IRE-RNA significantly changes the ΔH and ΔS to –38.1 ± 3.4 kJ. mol^{-1} and 34.5 ± 2.5 kJ. mol^{-1}, whereas for eIF4G·eIF4E IRE RNA complex to –45.1 ± 2.5 kJ. mol^{-1} and 17.2 ± 0.7 kJ. mol^{-1}, respectively. The binding free energy value was reported at 25 °C. Interestingly, ΔG value for the associ-

Table 1. Temperature dependence binding affinity of ferritin IRE RNA interaction with eIF4G and eIF4G·eIF4E determined by fluorescence titrations.

	K_d (nM)				
	5 °C	10 °C	15 °C	20 °C	25 °C
eIF4G·IRE	18.2 ± 1.1	27.3 ± 2.3	37.4 ± 2.5	49.3± 3.7	63.0 ± 4.3
eIF4G·IRE-Fe^{2+}	6.1 ± 0.4	8.3 ± 0.2	10.4 ± 0.3	13.0 ± 0.5	17.0 ± 0.8
eIF4G·eIF4E-IRE	9.1 ± 0.3	17.0 ± 0.6	25.4 ± 2.3	34.0 ± 2.6	46.3 ± 3.6
eIF4G·eIF4E-IRE-Fe^{2+}	4.0 ± 0.2	5.1 ± 0.1	6.7 ± 0.4	9.7 ± 0.3	13.0 ± 0.5

Table 2. Thermodynamic data of ferritin IRE binding to eIF4G and eIF4G·eIF4E determined by fluorescence titrations.

	ΔH	ΔS	ΔG
	kJ.mol^{-1}	J.mol^{-1}K^{-1}	kJ.mol^{-1}
eIF4G·IRE RNA	–42.6 ± 3.3	–11.5 ± 0.4	–39.2 ± 2.7
eIF4G·IRE RNA-Fe^{2+}	–38.1 ± 3.4	34.5 ± 2.9	–48.4 ± 4.2
eIF4G·eIF4E-IRE RNA	–54.6 ± 4.3	–43.2 ± 2.4	–41.7 ± 2.9
eIF4G·eIF4E-IRE RNA-Fe^{2+}	–45.1 ± 2.5	17.2 ± 0.7	–50.2 ± 2.7

ation of ferritin IRE with eIF4G or eIF4G·eIF4E complex increased significantly with addition of iron. We observed that the binding free energy and enthalpy changes are predominantly negative sign, favoring association of protein with mRNA. The sign and magnitude of thermodynamic parameters are primarily contributed for the involvement of binding forces between protein and RNA [37]. –ΔG values suggested that the complex formation at four different temperatures was feasible and the binding reaction was spontaneous. The negative ΔH value characterized the binding reaction as exothermic. Large negative ΔH value for the complex formation suggested the involvement of hydrogen bonds [37,38]. On the other hands a positive ΔS value was obtained for the eIF4G/IRE and eIF4G(eIF4E/IRE in the presence of iron indicated involvement of hydrophobic interactions. Therefore, our data concluded that the main acting forces are hydrogen bonds as well as hydrophobic interactions in eIF4G/IRE-RNA and eIF4G(eIF4E/IRE-RNA complex formation. Binding free energy, ΔG, for the eIF4G/IRE-RNA and eIF4G(eIF4E/IRE-RNA with addition of iron change to –48.4 ± 4.2 kJ. mol^{-1} and –50.2 ± 2.7 kJ. mol^{-1}, respectively, which corresponds to the change in the ΔG of binding by about 8.5 and 9.2, typical value for two additional noncovalent hydrogen bonds [39]. Enhancement in ΔG of binding for eIF4G(IRE RNA and eIF4G(eIF4E-IRE RNA in the presence of iron, suggest that Fe^{2+} promotes structural alterations in eIF4G/IRE and eIF4G(eIF4E/IRE-RNA complexes, allowing stable complex formation with translation initiation factors, subsequently upregulating protein synthesis.

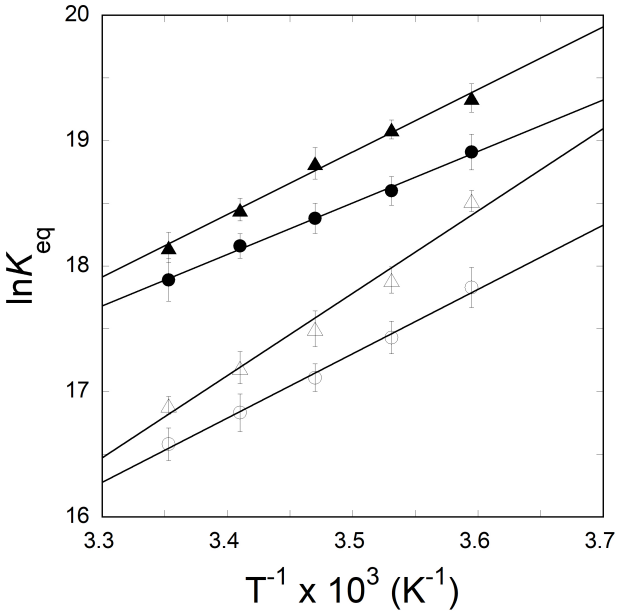

Fig. 9. Thermodynamics of ferritin IRE RNA interaction with the initiation factors described by the van't Hoff plot for eIF4G (—○—), eIF4G-Fe^{2+} (—●—), eIF4G·eIF4E (—△—), and eIF4G·eIF4E-Fe^{2+} (—▲—), respectively.

4. Discussion

This report for the first time shows the specificity of eIF4G by which ferritin IRE mRNA interact and stimulates capped/uncapped translation of structured mRNA. Iron increases the binding affinity of ferritin IRE to eIF4G, whereas decreases the ferritin IRE binding to IRP [4,21]. Thus, eIF4G-dependent IRE-mRNA translation elevates. To be able to respond quickly to any cellular iron changes, upregulation/repression of mRNA must change rapidly. Previous [4] report showed the eIF4F binds to IRE, and this binding performs crucial role for translation initiation of ferritin mRNA. Recent data reported [40], eIF4F/IRE binding correlates with the translational efficiency of ferritin mRNA. Berset *et al.* [19] showed that initiation factor eIF4G have three domains for RNA binding. If eIF4G domain responsible for RNA binding deleted, it directly

affects the *in vitro* and *in vivo* translation efficiency and binding affinity. Translation of capped/uncapped ferritin mRNA in eIF4F-depleted WG lysates showed more efficient in the presence of eIF4G compared to eIF4E, with the larger effect attributable to capped mRNA. Addition of eIF4G significantly enhances translation of ferritin luciferase reporter mRNA in depleted WG lysate. We show that ferritin mRNA was unable to bind with eIF4E. Addition of increasing amount of eIF4E did not influence the translation of ferritin mRNA in eIF4F-dependent wheat germ lysate. These results reveal that supplementation of eIF4G in depleted WG lysate restored translation, suggesting the involvement of eIF4G binding to ferritin IRE mRNA for protein synthesis.

To further understand these interactions, quantitative measurements were made between ferritin IRE mRNA and two subunits eIF4G and eIF4E. It has been shown that IRE binds with eukaryotic translation initiation factor eIF4F [4,31], but specificity of eIF4G binding and eIF4G-dependent translation efficiency had not been investigated. Present study provides direct evidence for the interaction of eIF4G with ferritin IRE RNA. Ferritin IRE RNA strongly binds to eIF4G as compared to eIF4E. Binding data showed that eIF4G contain single strong binding affinity for ferritin IRE. Our recent studies [30] using intrinsic protein fluorescence had shown that eIF4F bound to ferritin IRE tighter than eIF4G and noncompetitive binding for ferritin IRE and eIF4E. Binding data suggest that ferritin IRE forms complex with eIF4G following m7G cap/eIF4E complex formation, and this assembly with eIF4E might only involve in the initiation of protein synthesis of ferritin IRE, possibly 43S pre-initiation complex formation. Recently [30] interactions between eIF4F, IRE and m^7G cap have been demonstrated the non-competitive binding support the notion of IRE and m^7G cap binding on eIF4G and eIF4E. This selective binding to eIF4G was found to functionally drive expression of ferritin mRNA. This effect appears to depend on eIF4G/IRE interactions.

Temperature-dependent binding constant reveals that eIF4G/IRE RNA and eIF4G·eIF4E/IRE complex formation is enthalpy driven and entropy opposed. The strong interaction between initiation factor 4G and IRE is related with high ΔH of association (-42.6 ± 3.3 kJ.mol^{-1}). Presence of iron significantly changes the ΔH, ΔS, and ΔG values for the interaction of eIF4G and eIF4G·eIF4E with ferritin IRE. Iron enhances the affinity of eIF4G and eIF4G·eIF4E complex for IRE RNA about 4-fold; the ΔG value increased ~8.5 kJ.mol^{-1} and 9.2 kJ.mol^{-1} for the eIF4G and eIF4G·eIF4E/IRE with addition of iron. This change in ΔG (5–6 kJ.mol^{-1}) indicates the formation of additional H-bond, and salt bridge between protein and RNA molecule [39,41]. These data show that additional H-bonds further stabilized the ferritin IRE RNA/eIF4G complex formation. It has been reported that alteration of H-bonding involves overall conformation change of molecule [42]. eIF4G subunit responsible for the interaction with RNA through H-bonding, salt bridge, and van der Waals forces [20,43,44]. This RNA binding along with ribosomal attachment promotes efficient translation. eIF4E subunit directly interacts with mRNA cap and promotes initiation events through conformational change of eIF4E [45]. Interaction of ferritin IRE with eIF4F induces structural alteration in eukaryotic initiation factor 4F [30]. Consequently, these structural changes provide favorable positioning for stable complex formation for an effective eIF4G-dependent translation. Previously [21,46] reported that iron enhanced interaction of ferritin IRE with eIF4F, while increase dissociation of IRP from IRP/IRE-RNA complex, and subsequent enhance translation by forming more stable platform for further assembly of the initiation factors. Iron increases eIF4G/IRE complex binding affinity and facilitates assembly of other initiation factor binding for efficient mRNA translation. Taken together, these data provide insights into how eIF4G interacts with ferritin IRE and facilitates eIF4G-dependent translation. There are still much to be learned about the role of other initiation factors in iron translation regulation.

5. Conclusions

Ferritin IREs stem-loop structure specifically interacts with eIF4G subunit of eIF4F. eIF4G binding to the IRE RNA is enhanced by iron. Both equilibrium and thermodynamic of eIF4G binding to IRE-mRNA are controlled by iron and promote eIF4G-dependent protein synthesis. Thus, when free cellular iron levels enhance, rate of ferritin protein synthesis enhances more than the housekeeping protein, aconitase, because when iron levels lower, a larger fraction of ferritin IRE-mRNA molecules were inactivated by IRP interact than aconitase IRE molecules. Cellular iron ion destabilizes mRNA/IRP complexes competes with the stabilization conferred by hydrogen bonds between IRE RNA and eIF4G. Iron enhances the binding affinity of eIF/IRE complex and facilitates translational efficiency by forming a more stable platform for further assembly point of other initiation factor, demonstrating biological importance of this binding during cellular environment changes.

Abbreviations

IRE, iron responsive element; IRP, iron regulatory protein; WG, wheat germ; DWG, depleted wheat germ; eIF, eukaryotic initiation factor; UTR, untranslated region.

Author Contributions

MAK conceived and designed the experiments; performed the experiments; analyzed the data; contributed reagents and materials; wrote the paper.

Ethics Approval and Consent to Participate

Not applicable.

Acknowledgment

I thank Research, Innovation and Graduate Council, and College of Science, Alfaisal University for providing all necessary facilities.

Funding

This study was supported by grant from the Alfaisal University Research support, Riyadh, Saudi Arabia (IRG20413 to MAK).

Conflict of Interest

The author declares no conflict of interest.

References

[1] Piccinelli P, Samuelsson T. Evolution of the iron-responsive element. RNA. 2007; 13: 952–966.

[2] Rogers JT, Xia N, Wong A, Bakshi R, Cahill CM. Targeting the Iron-Response Elements of the mRNAs for the Alzheimer's Amyloid Precursor Protein and Ferritin to Treat Acute Lead and Manganese Neurotoxicity. International Journal of Molecular Sciences. 2019; 20: 994.

[3] Chen S, Olsthoorn RCL. Relevance of the iron-responsive element (IRE) pseudotriloop structure for IRP1/2 binding and validation of IRE-like structures using the yeast three-hybrid system. Gene. 2019; 710: 399–405.

[4] Ma J, Haldar S, Khan MA, Sharma SD, Merrick WC, Theil EC, *et al*. Fe2+ binds iron responsive element-RNA, selectively changing protein-binding affinities and regulating mRNA repression and activation. Proceedings of the National Academy of Sciences of the United States of America. 2012; 109: 8417–8422.

[5] Pantopoulos K. Iron metabolism and the IRE/IRP regulatory system: an update. Annals of the New York Academy of Sciences. 2004; 1012: 1–13.

[6] Kawahara M, Kato-Negishi M, Tanaka K. Amyloids: Regulators of Metal Homeostasis in the Synapse. Molecules. 2020; 25: 1441.

[7] Zhang P, Park HJ, Zhang J, Junn E, Andrews RJ, Velagapudi SP, *et al*. Translation of the intrinsically disordered protein α-synuclein is inhibited by a small molecule targeting its structured mRNA. Proceedings of the National Academy of Sciences of the United States of America. 2020; 117: 1457–1467.

[8] Costain G, Ghosh MC, Maio N, Carnevale A, Si YC, Rouault TA, *et al*. Absence of iron-responsive element-binding protein 2 causes a novel neurodegenerative syndrome. Brain. 2019; 142: 1195–1202.

[9] Ward RJ, Zucca FA, Duyn JH, Crichton RR, Zecca L. The role of iron in brain ageing and neurodegenerative disorders. The Lancet Neurology. 2014; 13: 1045–1060.

[10] Zecca L, Youdim MBH, Riederer P, Connor JR, Crichton RR. Iron, brain ageing and neurodegenerative disorders. Nature Reviews Neuroscience. 2004; 5: 863–873.

[11] Hare D, Ayton S, Bush A, Lei P. A delicate balance: Iron metabolism and diseases of the brain. Frontiers in Aging Neuroscience. 2013; 5: 1–19.

[12] Zhou ZD, Tan E. Iron regulatory protein (IRP)-iron responsive element (IRE) signaling pathway in human neurodegenerative diseases. Molecular Neurodegeneration. 2017; 12: 75.

[13] Zhang DL, Ghosh MC, Rouault TA. The physiological functions of iron regulatory proteins in iron homeostasis - an update. Frontiers in Pharmacology. 2014; 5: 124.

[14] Hershey JWB, Merrick WC. The pathway and mechanism of initiation of protein synthesis. Sonenberg N, Hershey JWB, and Mathews MB, eds. In Translational Control of Gene Expression (pp. 33–88). Cold Spring Harbor Laboratory Press: Cold Spring Harbor, New York. 2000.

[15] Sonenberg N. mRNA 5′ cap binding protein and control of cell growth. Cold Spring Laboratory Press: Cold Spring Harbor, NY. 1996.

[16] Merrick WC. Eukaryotic Protein Synthesis: still a Mystery. Journal of Biological Chemistry. 2010; 285: 21197–21201.

[17] Gingras A, Raught B, Sonenberg N. EIF4 Initiation Factors: Effectors of mRNA Recruitment to Ribosomes and Regulators of Translation. Annual Review of Biochemistry. 1999; 68: 913–963.

[18] Tarun SZ, Sachs AB. Association of the yeast poly(a) tail binding protein with translation initiation factor eIF-4G. The EMBO Journal. 1996; 15: 7168–7177.

[19] Berset C, Zurbriggen A, Djafarzadeh S, Altmann M, Trachsel H. RNA-binding activity of translation initiation factor eIF4G1 from *Saccharomyces cerevisiae*. RNA. 2003; 9: 871–880.

[20] Slepenkov SV, Korneeva NL, Rhoads RE. Kinetic Mechanism for Assembly of the m7GpppG·eIF4E·eIF4G Complex. Journal of Biological Chemistry. 2008; 283: 25227–25237.

[21] Khan MA, Walden WE, Goss DJ, Theil EC. Direct Fe2+ Sensing by Iron-responsive Messenger RNA·Repressor Complexes Weakens Binding. Journal of Biological Chemistry. 2009; 284: 30122–30128.

[22] Walden WE, Selezneva AI, Dupuy J, Volbeda A, Fontecilla-Camps JC, Theil EC, *et al*. Structure of Dual Function Iron Regulatory Protein 1 Complexed with Ferritin IRE-RNA. Science. 2006; 314: 1903–1908.

[23] Walden WE, Selezneva A, Volz K. Accomodating variety in iron-responsive elements: Crystal structure of transferrin receptor 1 B IRE bound to iron regulatory protein 1. FEBS Letters. 2012; 586: 32–35.

[24] Ke Y, Wu J, Leibold EA, Walden WE, Theil EC. Loops and Bulge/Loops in Iron-responsive Element Isoforms Influence Iron Regulatory Protein Binding. Journal of Biological Chemistry. 1998; 273: 23637–23640.

[25] Tibodeau JD, Fox PM, Ropp PA, Theil EC, Thorp HH. The upregulation of ferritin expression using a small-molecule ligand to the native mRNA. Proceedings of the National Academy of Sciences. 2006; 103: 253–257.

[26] Khan MA. Phosphorylation of translation initiation factor eIfiso4E promotes translation through enhanced binding to potyvirus VPg. ournal of Biochemistry. 2019; 165: 167–176.

[27] Khan MA, Miyoshi H, Gallie DR, Goss DJ. Potyvirus genome-linked protein, VPg, directly affects wheat germ *in vitro* translation: interactions with translation initiation factors eIF4F and eIFiso4F. Journal of Biological Chemistry. 2008; 283: 1340–1349.

[28] Khan MA, Miyoshi H, Ray S, Natsuaki T, Suehiro N, Goss DJ. Interaction of Genome-linked Protein (VPg) of Turnip Mosaic Virus with Wheat Germ Translation Initiation Factors eIFiso4E and eIFiso4F. Journal of Biological Chemistry. 2006; 281: 28002–28010.

[29] Khan MA, Goss DJ. Poly (a) binding protein enhances the binding affinity of potyvirus VPg to eukaryotic initiation factor eIF4F and activates *in vitro* translation. International Journal of Biological Macromolecules. 2019; 121: 947–955.

[30] Khan MA, Malik A, Domashevskiy AV, San A, Khan JM. Interaction of ferritin iron responsive element (IRE) mRNA with translation initiation factor eIF4F. Spectrochimica Acta Part a: Molecular and Biomolecular Spectroscopy. 2020; 243: 118776.

[31] Khan MA, Goss DJ. Poly(a)-Binding Protein Increases the Binding Affinity and Kinetic Rates of Interaction of Viral Protein Linked to Genome with Translation Initiation Factors eIFiso4F

and eIFiso4F·4B Complex. Biochemistry. 2012; 51: 1388–1395.
[32] Levine RL. Fluorescence-quenching studies of the binding of bilirubin to albumin. Clinical Chemistry. 1977; 23: 2292–2301.
[33] Khan MA, Muzammil S, Musarrat J. Differential binding of tetracyclines with serum albumin and induced structural alterations in drug-bound protein. International Journal of Biological Macromolecules. 2002; 30: 243–249.
[34] Gallie DR. Cap-Independent Translation Conferred by the 5′ Leader of Tobacco Etch Virus is Eukaryotic Initiation Factor 4G Dependent. Journal of Virology. 2001; 75: 12141–12152.
[35] Lomakin IB, Hellen CUT, Pestova TV. Physical Association of Eukaryotic Initiation Factor 4G (eIF4G) with eIF4a Strongly Enhances Binding of eIF4G to the Internal Ribosomal Entry Site of Encephalomyocarditis Virus and is Required for Internal Initiation of Translation. Molecular and Cellular Biology. 2000; 20: 6019–6029.
[36] Dix DJ, Lin PN, Kimata Y, Theil EC. The iron regulatory region of ferritin mRNA is also a positive control element for iron-independent translation. Biochemistry. 1992; 31: 2818–2822.
[37] Ross PD, Subramanian S. Thermodynamics of protein association reactions: forces contributing to stability. Biochemistry. 1981; 20: 3096–3102.
[38] Tayyab S, Sam SE, Kabir MZ, Ridzwan NFW, Mohamad SB. Molecular interaction study of an anticancer drug, ponatinib with human serum albumin using spectroscopic and molecular docking methods. Spectrochimica Acta Part a: Molecular and Biomolecular Spectroscopy. 2019; 214: 199–206.
[39] Kuntz ID, Chen K, Sharp KA, Kollman PA. The maximal affinity of ligands. Proceedings of the National Academy of Sciences. 1999; 96: 9997–10002.
[40] Khan MA, Domashevskiy AV. Iron enhances the binding rates and translational efficiency of iron responsive elements (IREs) mRNA with initiation factor eIF4F. PLoS ONE. 2021; 16: e0250374.
[41] Pace CN, Shirley BA, McNutt M, Gajiwala K. Forces contributing to the conformational stability of proteins. The FASEB Journal. 1996; 10: 75–83.
[42] Carberry SE, Rhoads RE, Goss DJ. A spectroscopic study of the binding of m7GTP and m7GpppG to human protein synthesis initiation factor 4E. Biochemistry. 1989; 28: 8078–8083.
[43] Tomoo K, Shen X, Okabe K, Nozoe Y, Fukuhara S, Morino S, *et al*. Structural Features of Human Initiation Factor 4E, Studied by X-ray Crystal Analyses and Molecular Dynamics Simulations. Journal of Molecular Biology. 2003; 328: 365–383.
[44] Marcotrigiano J, Burley SK. Structural biology of eIF4F: mRNA recognition and preparation in eukaryotic translation initiation. Advances in Protein Chemistry. 2002; 61: 269–297.
[45] Kiraga-Motoszko K, Niedzwiecka A, Modrak-Wojcik A, Stepinski J, Darzynkiewicz E, Stolarski R. Thermodynamics of Molecular Recognition of mRNA 5′ Cap by Yeast Eukaryotic Initiation Factor 4E. The Journal of Physical Chemistry B. 2011; 115: 8746–8754.
[46] Khan MA, Walden WE, Theil EC, Goss DJ. Thermodynamic and Kinetic Analyses of Iron Response Element (IRE)-mRNA Binding to Iron Regulatory Protein, IRP1. Scientific Reports. 2017; 7: 8532.